Detection of acute smoke-induced airway injury in a New Zealand white rabbit model using optical coherence tomography

Matthew Brenner
University of California—Irvine
Beckman Laser Institute
Irvine, California 92612
and
UC Irvine Medical Center
Pulmonary and Critical Care Division
Orange, California 92868

Kelly Kreuter
David Mukai
Tanya Burney
Shuguang Guo
Jianping Su
Sari Mahon
University of California—Irvine
Beckman Laser Institute
Irvine, California 92612

Andrew Tran
Lillian Tseng
Johnny Ju
UC Irvine Medical Center
Pulmonary and Critical Care Division
Orange, California 92868

Zhongping Chen
University of California—Irvine
Beckman Laser Institute
Irvine, California 92612

Abstract. Optical coherence tomography (OCT) is a micron scale high-resolution optical technology that can provide real-time *in vivo* images noninvasively. The ability to detect airway mucosal and submucosal injury rapidly will be valuable for a range of pulmonary applications including assessment of acute inhalation smoke and burn injury. OCT has the potential ability to monitor the progression of airway injury changes including edema, hyperemia, and swelling, which are critical clinical components of smoke-inhalation injury. New Zealand white male rabbits exposed to cold smoke from standardized unbleached burned cotton administered during ventilation were monitored for 6 h using a 1.8-mm diameter flexible fiberoptic longitudinal probe that was inserted through the endotracheal tube. The thickness of the epithelial, mucosal, and submucosal layers of the rabbit trachea to the tracheal cartilage was measured using a prototype superluminescent diode OCT system we constructed. OCT was able to detect significant smoke-injury-induced increases in the thickness of the tracheal walls of the rabbit beginning very shortly after smoke administration. Airway wall thickness increased to an average of 120% (±33%) of baseline values by 5 h following exposure. OCT is capable of providing real-time, noninvasive images of airway injury changes following smoke exposure. These studies suggest that OCT may have the ability to provide information on potential early indicators of impending smoke-inhalation-induced airway compromise.
 [DOI: 10.1117/1.2798637]

Keywords: imaging systems; medical imaging; fiber optics.

Paper 07030SSR received Jan. 19, 2007; revised manuscript received Mar. 6, 2007; accepted for publication Apr. 26, 2007; published online Oct. 29, 2007.

1 Introduction

Inhalation airway injury is a major cause of morbidity and mortality. Inhalation exposure risks include thermal, chemical, and toxic injuries, as well as secondary infectious complications. In inhalation burn victims, airway hyperemia, edema, sloughing, and necrosis are contributing pathophysiologic alterations that lead to critical airway compromise.[1,2] Management of inhalation burn injury patients remains difficult because respiratory symptoms and airway compromise may sometimes be delayed up to 2 to 5 days after exposure.[3,4] At the present time, there are no reliable methods to accurately determine which patients will proceed to develop life-threatening airway compromise following inhalation burn exposure. Assessment of hypoxemia and carboxyhemoglobin are indicators of more distal alveolar inhalation exposures and injury and may not correlate with proximal airway damage and impending airway risks. Therefore, physicians must rely on bronchoscopy and relatively rudimentary clinical findings to make critical decisions regarding prophylactic intubation and ventilatory support in the early period following burn and smoke exposure.[5–8] Development of a relatively noninvasive method for detecting and monitoring changes occurring in airway injury patients is a much needed clinical advance.

Advances in rapid acquisition high-resolution flexible fiberoptic optical coherence tomography (OCT) now offer the theoretical potential for obtaining repeated minimally invasive, real-time near histologic level optical imaging of airway epithelial, mucosal, and submucosal tissues for inhalation injury evaluation. The objective of this research was to develop methods and assess the feasibility of real-time, *in vivo* flexible fiberoptic OCT imaging in acute cold smoke-inhalation airway injury evaluation.

Address all correspondence to Matt Brenner, MD, Professor of Medicine, Pulmonary and Critical Care Division, UC Irvine Medical Center, Building 53, 119 Room 101 City Drive South, Orange, California 92868; Tel: 714–456–5150; Fax: 714–456–8349; E-mail: mbrenner@uci.edu; and Zhongping Chen, PhD, Professor of Biomedical Engineering, Beckman Laser Institute, 1002 Health Sciences Road East, UC Irvine, Irvine, California 92612; E-mail: Zchen@bli.uci.eduZ2chen@bli.uci.edu

1083-3668/2007/12(5)/051701/6/$25.00 © 2007 SPIE

2 Materials and Methods

2.1 *ARC Approval*

This protocol was approved by the University of California—Irvine AALAC approved ARC #2003-2397 and Department of Defense AFOSR 2004-0011A. All animals were treated in accordance with federal and state regulatory guidelines.

2.2 *General Preparation*

Fourteen male New Zealand white rabbits (7 controls, 7 smoke-inhalation animals) weighing 4.0±0.4 kg (Western Oregon Rabbit Company, Philomath, Oregon) were anesthetized with a 2:1 ratio of Ketamine HCl (100 mg/ml) (Ketaject, Phoenix Pharmaceutical Inc., St. Joseph, Michigan): Xylazine (20 mg/ml) (Anased, Lloyd Laboratories, Shenandoa, Iowa) at a dose of 0.75-cc/kg intramuscular (IM) using a 23-gauge, 5/8-in. needle. After the IM injection, a 23-gauge, 1-in. catheter was placed in the marginal ear vein to administer intravenous (IV) maintenance anesthetic of a 1:1:3 mixture of Ketamine:Xylazine:Saline (Ketamine 100 mg/ml:Xylazine 20 mg/ml) as a continuous infusion, at a rate of 0.17 ml/min. A dose of analgesic, Torbutrol 0.1 to 0.5 mg/kg subcutaneous (SQ), was given prior to intubation. The animals were intubated and mechanically ventilated ["ventilator 1"] (dual phase control respirator, model 613, Harvard Apparatus, Chicago, Illinois) at a respiratory rate of 32/min and a tidal volume of 60 cc and FiO_2 of 100%. A humidifier (Humid-Vent Mini Ref. 10011, Hudson RCI, Temecula, California) was positioned between the ventilator and endotracheal tube to prevent drying out of the mucosa, which could result in airway changes due to prolonged exposure to ventilated O_2 and not smoke. Upon completion of the experiment, the subjects were euthanized with an intravenous injection of Eutha-6 (1.0 to 2.0 cc) administered through the marginal ear vein.

2.3 *Systemic Arterial Blood Pressure, Blood Gas Analysis, and Co-Oximetry*

Femoral arterial and venous cutdowns were performed to collect blood samples and record systemic blood pressure. An 18-gauge catheter (C-PMA-400-FA, Cook Inc., Bloomington, Indiana) was inserted into the vein and artery, and a three way stopcock was placed on the ends. To measure systemic arterial pressure, a calibrated pressure transducer (TSD104A Transducer and MP100 WSW System, Biopac Systems, Inc., Santa Barbara, California) was connected to a PA extension set, which was then attached to the end of the stopcock. Blood was drawn from both the arterial and venous lines and measured by a blood gas analyzer (IRMA SL Series 2000 Blood Analysis System, Diametrics Medical Inc., St. Paul, Minnesota) in order to obtain arterial and venous blood gas analysis, respectively. On-site co-oximetry measurements (AVOXimeter 4000, AVOX Systems, San Antonio, Texas) were conducted to measure oxy hemoglobin, carboxy hemoglobin (CoHgb), methemoglobin fractions, and total hemoglobin. Specifically, the COHgb levels were analyzed to confirm that the animal had received significant smoke exposure. The co-oximeter was calibrated with rabbit blood by the manufacturer for research purposes of these studies.

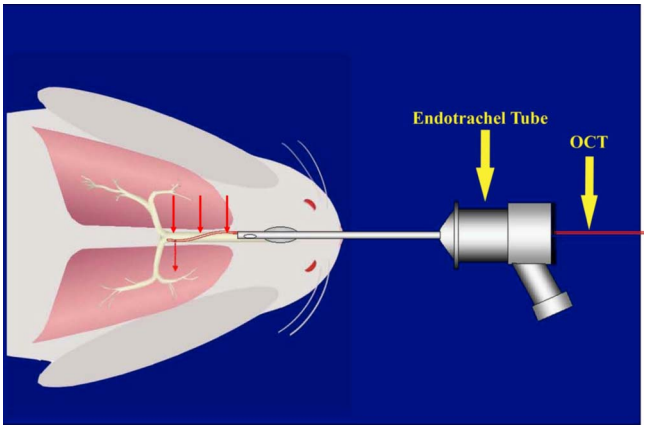

Fig. 1 Experimental setup of the intubated subject. The OCT probe has been inserted though the endometrial tube into the distal trachea or proximal bronchi and is held in position throughout the study using a constricting gasket adapter. The arrows show areas to be imaged.

2.4 *Administration of Smoke*

To administer smoke to the animals, modifications of a standard rabbit smoke-inhalation animal model was used.[9] Seventy grams of unbleached cotton was burned in a modified bee smoker (Smoke Stack Smoker #644, Brushy Mountain Bee Farm, Moravian Falls, North Carolina) for approximately 20 min. The bee smoker was then connected to the inlet port of the mechanical ventilator with the tidal volume and ventilation rate set at 700 ml and 25 breaths per minute, respectively. A Mylar Douglas bag (model 6060, Hans Rudolph, Kansas City, Missouri) was connected to a second "smoke exposure" ventilator [ventilator 2 (also a dual phase control respirator, model 613, Harvard Apparatus, Chicago, Illinois)] via the multiport valve to the output port to actively fill the bag with smoke from the bee smoker and over 25 L of smoke was collected. The Mylar bag was then connected to the inlet port of the smoke exposure ventilator and set to a tidal volume of 60 ml and a ventilation rate of 18 breaths per minute to deliver the (now cool) smoke-filled contents of the Douglas bag to the rabbit in a controlled manner. The rabbit was disconnected from the regular ventilator (1) circuit and connected to the smoke ventilator (2) for exposure. Exposure was achieved by giving the animal repetitive alternate increments of 18 breaths of smoke, followed by 100% oxygen (accomplished by switching between the traditional ventilator setup and the smoke ventilator). The animals were administered either 0 (controls) or 90 breaths (high dose) of smoke. Measurements of blood and concurrent OCT were obtained at preexposure, and 15, 30, 60, 90, 120, 180, 240, 300, and 360 min postexposure (though the OCT catheter was left in position in the airway throughout the period and was capable of taking continuous OCT images if desired (Fig. 1).

2.5 *OCT System and Probes*

The OCT system used in this study contains a superluminescent diode source that delivers an output power of 10 mW at a central wavelength of 1310 nm with a full width at half maximum (FWHM) of 80 nm, resulting in approximately 10-μm axial resolution.

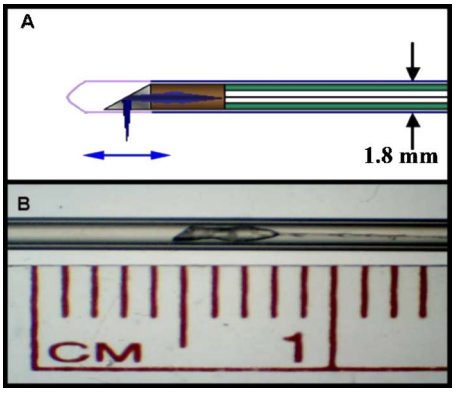

Fig. 2 Translational flexible fiberoptic probes used in OCT smoke-induced airway injury measurements. (a) Top figure shows a schematic of the flexible fiberoptic probe with external diameter 1.8-mm outer sheath containing a single-mode optical fiber encased in protective coating, connected to 0.7-mm GRIN lens and reflecting prism. The longitudinal direction of imaging is obtained using a linear motor to move the internal components as shown, resulting in cross-sectional images of 16 mm. (b) Photograph of an actual probe constructed for use in this study revealing the components described above. Centimeter ruler included for size scale.

In the reference arm, a rapid-scanning optical delay line is used that employs a grating to control the phase and group delays separately so that no phase modulation is generated when the group delay is scanned. The phase modulation is generated through an electrooptic phase modulator that produces a carrier frequency. The axial line scanning rate is 500 Hz, and the modulation frequency of the phase modulator is 500 kHz. Reflected beams from the two arms are recombined in the interferometer and detected on a photodetector. The detected optical interference fringe intensity signals are bandpass filtered at the carrier frequency. Resultant signals are then digitized with an analog-digital converter that performs 12-bit-at-5-MHz signal conversion and transferred to a computer where the structural image is generated.[10,11]

Flexible fiber optic OCT probes were constructed from single-mode fiber (ThorLabs, Newton, New Jersey). The bare ended fiber was attached to a 0.7-mm diameter gradient index (GRIN) lens (NSG America, Irvine, California), using optical adhesive (Dymax Co., Torrington, Connecticut) under a microscope. A right angle light path was achieved using a 0.7-mm prism. The probe was placed in fluorinated ethylene propylene tubing (17-gauge thin wall, Zeus, Orangeburg, South Carolina) for added fiber support (Fig. 2).

A linear motor (Newport Instruments, Irvine, California) was used to drive the coated flexible fiberoptic distally and proximally along the length of the probe within the sheath, moving the GRIN lens and prism imaging components within the sheath to obtain linear images along the long axis of the trachea and bronchi. Axial scans were obtained every 10 μm along the length of the probe during 16-mm long scan sweeps. A 16-mm scan is obtained in 3.2 sec. Translational imaging has a number of distinct theoretical advantages over rotational scanning methods for initial investigations in relatively large lumen sites such as trachea and proximal bronchi.

2.6 *Airway Thickness Measurements*

Airway thickness was measured as the distance between the epithelial surface and the surface of landmark submucosal cartilaginous rings in the trachea and bronchi and includes epithelial, mucosal, submucosal, and glandular tissues above the cartilage. All measurements were obtained by two independent researchers (JJ, LT) who were blinded to all clinical information. Airway thickness measurements were taken at as many landmark cartilaginous rings as could be seen in an individual animal (generally three to five cartilage ring sites per animal) as shown in Fig. 3. Measurements of the airway thickness at the landmark rings were obtained at baseline and at each specified period following inhalation injury. The percentage of change from baseline was calculated for each airway thickness measurement at every time point. Values were then averaged for all airway thickness measurements within a given animal at each specified point.

2.7 *Statistical Analysis*

Analysis of variance by groups was performed on the changes in airway thickness in the smoke-inhalation versus control animals at the time points before and after exposure. A $p < 0.05$ two-tailed probability was considered a significant difference.

3 Results

To ensure that the rabbits received adequate smoke, we verified blood COHgb levels using co-oximetry and observed values of 1.6 to 18.3%. Translational (longitudinal) images 16-mm long were obtained from the probe in the lower trachea and proximal bronchi from preexposure and over a period of 6 h following smoke exposure. The 16-mm longitudinal sweep distance provided images with easily recognizable landmarks that could be followed continuously throughout the experimental course. Depth of penetration was approximately 1.6 mm, which allowed visualization of the full depth of the airways in the rabbit to well below the surface of the cartilaginous tracheal and bronchial rings (Fig. 3).

In some animals, dramatic increases in thickness of the airway could be seen beginning at intervals as short as 5 min following smoke exposure. However, there was marked variability in the degree and timing of changes across the group of smoke-exposed animals. In some animals no significant changes were seen at all, while in others, an increase of average thickness of as much as 260% developed. In contrast, in the control animals, minimal changes were seen in the majority of animals; though as a group there was a tendency toward some increase in overall airway layer thickness over time in these intubated, ventilated animals (Fig. 4).

Overall, there was a significant increase in the thickness of mucosa of those animals that received smoke, when compared to those animals that did not (Table 1). On average, airway layer thickness increased from baseline to 78.5±38% [standard error of mean (SEM)] above baseline at 30 min, peaking at a mean of 120±33% (SEM) above baseline at 5 h postexposure in the smoke-treated group ($p < 0.05$ compared to baseline and compared to controls). In comparison, the control group showed an 11.4±8.7% (SEM) increase at 30 min, with the peak of 39.2±24% (SEM) increase at 6 h (Fig. 4).

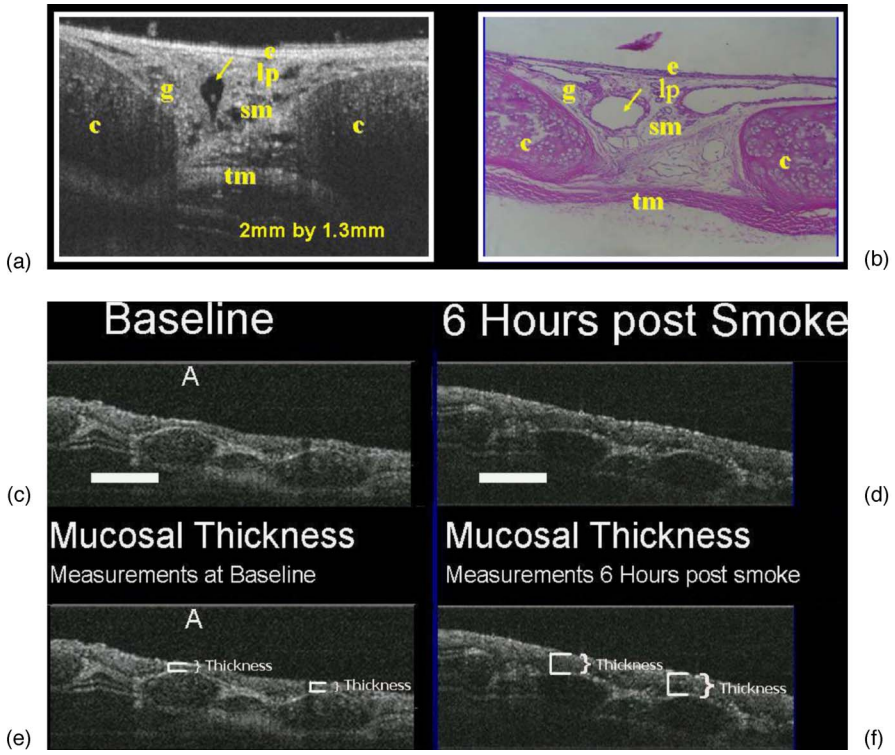

Fig. 3 Example of longitudinal OCT image of rabbit trachea (a) compared to histologic image shown (b). Epithelium (*e*), glands (*g*), cartilage (*c*), submucosal layers (*sm*), lamina propria (*lp*), and muscularis (L*m*) are clearly seen (Ref. 21). *In vivo* longitudinal images of rabbit trachea at baseline [(c) and (e)] and 6 h following inhalational smoke exposure [(d) and (f)]. Marked increase in the thickness of the epithelial, mucosal, and submucosal layers are evident, particularly visible above the cartilage rings. (e) and (f) images demonstrate the measurement methods for determining airway thickness above each tracheal ring for the images obtained in (c) and (d), respectively.

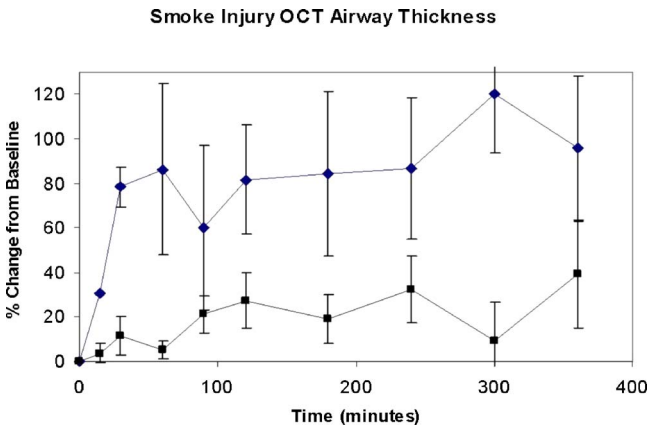

Fig. 4 Percentage of change in baseline of airway thickness determined by OCT versus time (minutes) following smoke-inhalation exposure compared to controls. Statistically significant increases in airway thickness are seen that begin very early following smoke exposure. No significant changes from baseline are detected in the control animals. Average change in airway thickness was greater than 120% compared to baseline by 5 h following smoke exposure.

Table 1 Change in airway thickness following smoke exposure.

Time (minutes)	Smoke animals (% change from baseline)	SEM	Control animals (% change from baseline)	SEM
0	-	-	-	-
15	30	9	4	5
30	78	38	11	9
60	86	37	5	4
90	60	25	21	8
120	82	37	27	12
180	84	32	19	11
240	86	27	32	15
300	120	33	9	17
360	96	24	39	24

Animals tolerated the 6 h of F-OCT monitoring well, and no significant complications were seen from the OCT catheter.

4 Discussion

This study demonstrates that OCT was able to detect significant changes in airway thickening occurring following smoke-inhalation injury *in vivo* in a clinically relevant animal model. The ability of flexible fiberoptic OCT to be performed repeatedly and reliably in a noncontact minimally invasive fashion attests to the potential value in this important clinical application. The feasibility of the methodology as well as the capabilities of the technology were demonstrated.

We utilize a translationally scanning 1.8-mm diameter probe with a long sweep distance setting (16 mm) to obtain easily recognizable, measurable images of the longitudinal cross section of the proximal lower airways in this rabbit model. The airway thickness could be readily assessed quantitatively and easily identifiable cartilaginous landmarks could be repeatedly and reproducibility located. Statistically and clinically significant changes in the thickening of the airway were seen in those animals that received smoke when compared to control animals that were treated in a similar manner but did not receive smoke exposure. Most importantly, immediately after sacrifice when airway observation by OCT was performed and when subsequent histologic evaluation was performed, the swelling that had been seen with OCT was no longer evident. This caused us to believe that the swelling we observed was due to primarily to hyperemia rather than edema, inflammation, or necrosis. Previous studies[1,2,12,13] have demonstrated that the very early changes examined in these studies consist primarily of hyperemia and edema—changes that may be lost during preparation of histologic specimens. These findings are consistent with earlier reports of the events associated with acute cold smoke-inhalation injury in the Bidani cotton smoke animal model[9] and in early findings in patients following acute inhalation smoke injury. Future studies will be needed to determine whether the very early changes that we are able to detect on OCT correlate with the extent of later injury and are predictive of development of life-threatening airway complications that occur at later times following exposure.

Despite its frequent clinical use, early standard bronchoscopy with or without invasive biopsy may not accurately reveal the extent of impending airway edema that often develops, including vessel hyperemia, edema, and sloughing of tracheal ciliated columnar epithelium.[2,13,14] From within the lumen of the airway during bronchoscopy, it is difficult to determine the presence or extent of airway mucosal swelling, particularly in the early phases following inhalation burn injury, and it is not possible to make any quantitative assessment of airway edema. The ability to obtain this information using OCT (possibly with optical Doppler tomography) without invasive biopsies (on a repeated basis) could lead to improved patient care, allow more complete monitoring of inhalation injury, provide a method for assessing response to therapy, and could potentially be used as a sensitive tool for determining the effectiveness of proposed therapeutic interventions. In future studies, the ability to assess collagen disruption with polarization sensitive OCT in the airways of thermally injured burn patients might be important areas for investigation as well.[15] Thus, OCT may provide much more direct information on proximal airway thermal and toxic injury than can be obtained by other methods available at this time.

There are a number of limitations to the conclusions that can be drawn from this study. First, there was substantial variability in the overall injury response and airway changes seen in the smoke-exposed animals. The reasons for this variability are uncertain at this time. Possible factors may include regional differences in the airflow and deposition patterns of the smoke as applied in this animal model, variable biological responses inherent within the animals, or other mechanical factors that we have not identified. Because no significant changes were seen in any of the control animals, we do not believe that the variability seen is due to experimental conditions other than smoke exposure or technical limitations of the OCT techniques and measurement methods, but rather due to true variability in airway pathophysiologic changes, as a result of smoke exposure. The degree of COHgb elevation seen in our animal models was also variable (1.6 to 18.3%), and considerably lower than those levels reported by Bidani,[9] whose group administered the smoke directly from the smoking chamber into the ventilator (rather than through a Douglas bag). This may indicate a lower-level exposure in our animals that may account for some of these findings. Second, because there are no postmortem OCT or histopathologic changes seen to correlate with these acute *in vivo* OCT injury findings, the accuracy of the OCT imaging and fidelity of the images to underlying *in vivo* pathologic changes that occurred cannot be confirmed with certainty. Furthermore, we examined very acute early injury changes, up to 6 h following exposure. Many of the most significant changes manifest at 24 h and later.[9] Longer term studies and higher dose exposures will clearly be needed to confirm and extend the current findings. Most importantly, the relationship between the early changes seen in these studies and the ultimate extent of airway injury developing over time needs to be determined. OCT should allow us to study this question.

The animals tolerated the presence of the flexible fiberoptic probe without difficulties. Care was taken to ensure that the probes were not in direct contact with the mucosal surface where they could potentially block the inhaled smoke from contacting the airway wall during administration, could potentially injure airway mucosa, or affect development of edema or hyperemia. Because the animals were anesthetized and mechanically ventilated, probe position remained stable throughout most of the studies. A number of methods could be developed in the future for ensuring stability of the probe location in longer-term animal studies or patients while avoiding the potential problems listed above. From a technical standpoint, OCT equipment, acquisition methods, functional OCT capabilities, and OCT probe technology are advancing rapidly.[16–20] Ultrahigh-resolution, three-dimensional, ultrafast acquisition may further enhance the capabilities of OCT for inhalation airway injury assessment.[16]

5 Conclusions

This study demonstrates that minimally invasive flexible fiberoptic OCT assessment of aspects of acute smoke-induced airway injury is feasible. Changes in epithelial, mucosal, and

submucosal airway structures were evident extremely early following exposure to cold smoke. Future studies will be needed to confirm and extend these very promising preliminary *in vivo* OCT inhalation airway injury findings and to determine causes for potential regional and individual variability in response to smoke exposure. Most importantly, longer-term studies assessing the relationship between acute airway changes and subsequent development of later airway compromise will be very important in animal models as well as patients with inhalation burn injury.

Acknowledgments

We would like to thank Emily Brenner for technical illustrations and Amit Uppal for assistance with measurements and experimental assistance. This work was supported by the Department of Defense under Grant No. FA 9550-04-1-0101.

References

1. R. A. Cox, A. S. Burke, K. Soejima, K. Murakami, J. Katahira, L. D. Traber, D. N. Herndon, F. C. Schmalstieg, D. L. Traber, and H. K. Hawkins, "Airway obstruction in sheep with burn and smoke inhalation injuries," *Am. J. Respir. Cell Mol. Biol.* **29**(3 Pt. 1), 295–302 (2003).
2. D. L. Traber, H. A. Linares, D. N. Herndon, and T. Prien, "The pathophysiology of inhalation injury—a review," *Burns Incl Therm Inj* **14**(5), 357–364 (1988).
3. R. L. Cecil, L. Goldman, and J. C. Bennett, *Cecil Textbook of Medicine*, W. B. Saunders, Philadelphia (2000).
4. D. R. Thorning, M. L. Howard, L. D. Hudson, and R. L. Schumacher, "Pulmonary responses to smoke inhalation: Morphologic changes in rabbits exposed to pine wood smoke," *Hum. Pathol.* **13**(4), 355–364 (1982).
5. R. L. Sheridan, "Airway management and respiratory care of the burn patient," *Int. Anesthesiol. Clin.* **38**(3), 129–145 (2000).
6. T. Muehlberger, D. Kunar, A. Munster, and M. Couch, "Efficacy of fiberoptic laryngoscopy in the diagnosis of inhalation injuries," *Arch. Otolaryngol. Head Neck Surg.* **124**(9), 1003–1007 (1998).
7. M. J. Masanes, C. Legendre, N. Lioret, R. Saizy, and B. Lebeau, "Using bronchoscopy and biopsy to diagnose early inhalation injury. Macroscopic and histologic findings," *Chest* **107**(5), 1365–1369 (1995).
8. M. J. Masanes, C. Legendre, N. Lioret, D. Maillard, R. Saizy, and B. Lebeau, "Fiberoptic bronchoscopy for the early diagnosis of subglottal inhalation injury: Comparative value in the assessment of prognosis," *J. Trauma* **36**(1), 59–67 (1994).
9. A. Bidani, H. K. Hawkins, C. Z. Wang, and T. A. Heming, "Dose dependence and time course of smoke inhalation injury in a rabbit model," *Lung* **177**(2), 111–122 (1999).
10. N. Hanna, D. Saltzman, D. Mukai, Z. Chen, S. Sasse, J. Milliken, S. Guo, W. Jung, H. Colt, and M. Brenner, "Two-dimensional and 3-dimensional optical coherence tomographic imaging of the airway, lung, and pleura," *J. Thorac. Cardiovasc. Surg.* **129**(3), 615–622 (2005).
11. N. M. Hanna, W. Waite, K. Taylor, W. G. Jung, D. Mukai, E. Matheny, K. Kreuter, P. Wilder-Smith, M. Brenner, and Z. Chen, "Feasibility of three-dimensional optical coherence tomography and optical Doppler tomography of malignancy in hamster cheek pouches," *Photomed. Laser Surg.* **24**(3), 402–409 (2006).
12. K. Murakami and D. L. Traber, "Pathophysiological basis of smoke inhalation injury," *News Physiol. Sci.* **18**, 125–129 (2003).
13. D. N. Herndon, R. E. Barrow, H. A. Linares, R. L. Rutan, T. Prien, L. D. Traber, and D. L. Traber, "Inhalation injury in burned patients: Effects and treatment," *Burns Incl Therm Inj* **14**(5), 349–356 (1988).
14. P. I. Ramzy, J. P. Barret, and D. N. Herndon, "Thermal injury," *Crit. Care Clin.* **15**(2), 333–352, ix (1999).
15. S. M. Srinivas, J. F. de Boer, H. Park, K. Keikhanzadeh, H. E. Huang, J. Zhang, W. Q. Jung, Z. Chen, and J. S. Nelson, "Determination of burn depth by polarization-sensitive optical coherence tomography," *J. Biomed. Opt.* **9**(1), 207–212 (2004).
16. J. G. Fujimoto, "Optical coherence tomography for ultrahigh resolution in vivo imaging," *Nat. Biotechnol.* **21**(11), 1361–1367 (2003).
17. Z. Chen, T. E. Milner, X. Wang, S. Srinivas, and J. S. Nelson, "Optical Doppler tomography: Imaging in vivo blood flow dynamics following pharmacological intervention and photodynamic therapy," *Photochem. Photobiol.* **67**(1), 56–60 (1998).
18. T. Gambichler, G. Moussa, M. Sand, D. Sand, P. Altmeyer, and K. Hoffmann, "Applications of optical coherence tomography in dermatology," *J. Dermatol. Sci.* **40**(2), 85–94 (2005).
19. T. D. Wang and J. Van Dam, "Optical biopsy: A new frontier in endoscopic detection and diagnosis," *Clin. Gastroenterol. Hepatol.* **2**(9), 744–753 (2004).
20. Y. Zhao, Z. Chen, Z. Ding, H. Ren, and J. S. Nelson, "Real-time phase-resolved functional optical coherence tomography by use of optical Hilbert transformation," *Opt. Lett.* **27**(2), 98–100 (2002).
21. S. Han, N. H. El-Abbadi, N. Hanna, U. Mahmood, R. Mina-Araghi, W. G. Jung, Z. Chen, H. Colt, and M. Brenner, "Evaluation of tracheal imaging by optical coherence tomography," *Respiration* **72**(5), 537–541 (2005).